

Spin quantum computation in silicon nanostructures

S. Das Sarma

*Condensed Matter Theory Center, Department of Physics,
University of Maryland, College Park, MD 20742-4111*

Rogério de Sousa

*Department of Chemistry and Pitzer Center for Theoretical Chemistry,
University of California, Berkeley, CA 94720-1460*

Xuedong Hu

Department of Physics, University at Buffalo, SUNY, Buffalo, NY 14260-1500

Belita Koiller

*Instituto de Física, Universidade Federal do Rio de Janeiro,
Cx. Postal 68.528, Rio de Janeiro, 21945-970, Brazil*

Proposed silicon-based quantum-computer architectures have attracted attention because of their promise for scalability and their potential for synergetically utilizing the available resources associated with the existing Si technology infrastructure. Electronic and nuclear spins of shallow donors (e.g. phosphorus) in Si are ideal candidates for qubits in such proposals because of their long spin coherence times due to their limited interactions with their environments. For these spin qubits, shallow donor exchange gates are frequently invoked to perform two-qubit operations. We discuss in this review a particularly important spin decoherence channel, and bandstructure effects on the exchange gate control. Specifically, we review our work on donor electron spin spectral diffusion due to background nuclear spin flip-flops, and how isotopic purification of silicon can significantly enhance the electron spin dephasing time. We then review our calculation of donor electron exchange coupling in the presence of degenerate silicon conduction band valleys. We show that valley interference leads to orders of magnitude variations in electron exchange coupling when donor configurations are changed on an atomic scale. These studies illustrate the substantial potential that donor electron/nuclear spins in silicon have as candidates for qubits and simultaneously the considerable challenges they pose. In particular, our work on spin decoherence through spectral diffusion points to the possible importance of isotopic purification in the fabrication of scalable solid state quantum computer architectures. We also provide a critical comparison between the two main proposed spin-based solid state quantum computer architectures, namely, shallow donor bound states in Si and localized quantum dot states in GaAs.

PACS numbers: 03.67.Lx, 71.55.Cn

I. INTRODUCTION

During the past decade, the study of quantum computing and quantum information processing has generated widespread interest among physicists from areas ranging from atomic physics, optics, to various branches of condensed matter physics [1, 2]. The key thrust behind the rush toward a working quantum computer (QC) is the development of a quantum algorithm that can factorize large numbers exponentially faster than any available classical algorithm [3]. This exponential speedup is due to the intrinsic quantum parallelism in the superposition principle and the unitary evolution of quantum mechanics. It implies that a computer made up of entirely quantum mechanical parts (qubits), whose evolution is governed by quantum mechanics, would be able to carry out prime factorization of large numbers that is prohibitively time-consuming in classical computation, thus revolutionizing cryptography and information theory. Since the invention of Shor's factoring algorithm, it has also been shown that error correction can be done to a quantum system [4], so that a practical QC does not have to be forever perfect to be useful, as long as quantum error corrections can be carried out on the QC. These two key mathematical developments have led to the creation of the new interdisciplinary field of quantum computation and quantum information.

Many physical systems have been proposed as candidates for qubits in a QC. Among the more prominent examples are electron or nuclear spins in semiconductors [5, 6], including electron spin in semiconductor quantum dots [7, 8] and donor electron or nuclear spins in semiconductors [9, 10, 11]. The donor-based QC schemes are particularly interesting because all donor electron wavefunctions in a semiconductor are identical, and because doping makes a natural connection between quantum mechanical devices and the more traditional microelectronic devices: Doping in semiconductors has had significant technological impact for the past fifty years and is the basis of the existing microelectronics technology. As transistors and integrated circuits decrease in size, the physical properties of the devices are becoming sensitive to the actual configuration of impurities [12]. In this context, the important proposal of donor-based silicon quantum computer (QC) by Kane [9], in which the nuclear spins of the monovalent ^{31}P impurities in Si are the qubits, has naturally created considerable interest in revisiting all aspects of the donor impurity problem in silicon, particularly in the Si: ^{31}P system.

In principle, both electron spin and orbital degrees of freedom can be used as qubits in semiconductor nanostructures. For example, electron orbital dynamics is quantized into discrete "atomic-like" levels (on meV energy scale with a Bohr radius of the order of 10 nm) in semiconductor quantum dots, and two such quantized quantum dot levels could form the quantum two-level system needed for a qubit [13]. A great advantage of such orbital (or equivalently, charge) qubits is that qubit-specific measurements are relatively simple since one is essentially measuring single charge states, which is a well-developed experimental technique through single-electron transistors (SET) or equivalent devices [14]. A major disadvantage of solid state charge qubits is that these orbital states are highly susceptible to interactions with the environment (which, in particular, contains all the stray or unintended charges inevitably present in the device), and the decoherence time is generally far too short (typically picoseconds to nanoseconds) for quantum error correction to be useful. A related problem is that inter-qubit coupling, which is necessary for the implementation of two-qubit gate operations essential for quantum computation, is often the long-range dipolar coupling for charge qubits. This makes it difficult to scale up the architecture, since decoherence grows with the scaling-up as more and more qubits couple to each other via the long-range dipolar coupling. Additional decoupling techniques have to be applied to ensure selective gate operations [15], and to control decoherence due to long range couplings [16]. Since scalability is thought to be the main advantage of solid state QC architectures, little serious attention has so far been paid to orbital qubit based quantum computation in semiconductor nanostructures due to its probably unscalable decoherence and entanglement properties.

Spin qubits in semiconductor nanostructures have complementary advantages (and disadvantages) compared with charge qubits based on quantized orbital states. A real disadvantage of spin qubits is that a single electron spin is difficult to measure, although there is no fundamental principle against the measurement of a Bohr magneton. The great advantage of spin qubits is the very long spin coherence times, which even for electron spins can be milliseconds (microseconds) in silicon (GaAs) at low temperatures. This six orders of magnitude coherence advantage in spin qubits over charge qubits has led to electron spin qubits in GaAs quantum dots and in P donor levels in silicon (as well as SiGe quantum structures) as the QC architectures of choice for the solid state community. In addition to the coherence advantage, spin qubits also have a considerable advantage that the exchange gate, which provides the inter-qubit coupling, is exponentially short-ranged and nearest-neighbor in nature, thus allowing precise control and manipulation of two-qubit gates. There is no fundamental problem arising from the scaling-up of the QC architecture since exchange interaction couples only two nearest-neighbor spin qubits independent of the number of qubits. In this review we provide a brief perspective on spin qubits in silicon with electron spins in shallow P donor levels in Si being used as qubits.

Although experimental progress in semiconductor-based solid state QC schemes has been slow to come during the past five years, they are still often considered promising in the long term because of their perceived scalability advantages. After all, the present computer technology is based on semiconductor integrated circuits with ever smaller

feature size. Therefore, semiconductor nanostructure-based QC architectures should in principle be scalable using the existing microelectronics technology. However, it still remains to be demonstrated whether and how the available (classical) semiconductor technology can help the scaling up of a quantum coherent QC architecture. For the spin qubits in silicon, for example, the key issues include clarifications of spin quantum coherence properties in the solid state environment, physical approaches to manipulate and entangle spins, fabrication of devices with atomic-scale precision, and measurement of single spins. In the following, we review our work on two of these important issues: donor electron spin coherence and spin interaction in silicon.

II. SPIN COHERENCE IN SILICON NANOSTRUCTURES

Before the seminal concept of quantum error correction was introduced in 1995 [4], it was widely believed that quantum computation, even as a matter of principle, is quite impossible since all quantum states decohere due to interaction with the environment, and such decoherence was thought to be fatal to QC operations. Although the quantum error correction principle has shown that a certain degree of decoherence can be corrected in QC algorithms, one still has severe limits on the amount of tolerable decoherence for feasible QC operations. The question of decoherence is therefore of paramount importance for any form of quantum computing architecture, including the spin-based proposals. Estimates of exchange coupling and various analysis of adiabatic operation of the exchange gates in quantum dots [17] suggest that the exchange gate duration is unlikely to be shorter than 100 ps—adiabaticity is likely to be compromised for shorter pulse times leading to loss of qubit fidelity. Hence spin coherence times at least of the order of microseconds are necessary to satisfy the criteria of fault-tolerance (10^4 reliable quantum gate operations during the coherence time [1]). Non-ideal situations encountered in real devices will probably require even longer coherence times. Here we argue that the possibility of using nuclear-spin-free samples of silicon through isotopic purification together with the small spin-orbit coupling in silicon makes Si one of the most promising host materials with respect to electron spin coherence. As we show below, both adiabaticity (i.e. “slow” gate operation) and fault tolerance (i.e. “fast” gate operation) are more easily satisfied in Si donor electron spins than in GaAs quantum dots.

The simplest description of electron spin coherence is to consider characteristic time scales T_1 and T_2 [18], which are respectively defined as the decay times of spin magnetization parallel (the so-called longitudinal spin relaxation time T_1) and perpendicular (the so-called transverse spin dephasing time T_2) to an external magnetic field. All processes contributing to T_1 require energy exchange with the lattice (via phonon emission, for example). These T_1 relaxation processes also contribute to the dephasing time T_2 , hence the inequality $T_2 \leq 2T_1$ [19]. However, often one finds $T_2 \ll T_1$ due to the importance of dephasing mechanisms that do not involve energy relaxation, thus contributing exclusively to T_2 decay. This is exactly the case for a Si:P donor electron spin. In this system T_1 can be as long as 10^3 seconds [20] (measured for $B = 0.3$ T – we note that $T_1 \propto B^{-5}$ at low temperatures due to phonon matrix element and phase space considerations [20]), while T_2 detected by spin echo decay is of the order of 10^{-4} seconds [21]. The reason why T_1 is so long in silicon nanostructures is two fold: (1) Spin flips mediated by spin-orbit coupling and the electron-phonon interaction are strongly suppressed for localized electrons [22] due to energy-momentum conservation constraints, and (2) spin-orbit coupling in silicon is significantly weaker than in other popular semiconductors [23] (such as III-V compounds, where T_1 is of the order of nanoseconds for conduction electrons [5]). This observation, together with the fact that one should expect $T_2 = 2T_1$ in isotopically purified ^{28}Si (see below), indicates that silicon is one of the most attractive materials for coherent spin manipulation.

It was discovered a long time ago [24] that the dipolar fluctuation of lattice nuclear spins is responsible for electron spin phase fluctuations, leading to significant suppression of T_2 , an effect usually denoted spectral diffusion. Here each nuclear spin produces a different hyperfine shift in the electron Zeeman frequency. Because the nuclei are coupled to each other via magnetic dipolar interaction leading to nuclear spin flip-flop transitions, the total hyperfine field at the localized electron fluctuates and leads to time-dependent noise in the electron spin Zeeman frequency and its consequent decoherence. Below we summarize a microscopic theory for this spectral diffusion effect which was proposed by two of us [25, 26] and recently verified experimentally [27, 28].

Silicon has three stable isotopes: ^{29}Si has nuclear spin quantum number $I = 1/2$ and a natural abundance equal to 4.68%. ^{28}Si and ^{30}Si are spin-0 and hence do not contribute to spectral diffusion. Nuclear isotope engineering [27, 28] can systematically reduce the amount of ^{29}Si (“the isotopic purification”), thus raising an important theoretical question on how T_2 depends on the fraction of ^{29}Si present in the sample. (We note that T_2 due to spectral diffusion becomes infinitely long as the fraction of ^{29}Si in the sample approaches zero.) To address this question, we consider a truncated Hamiltonian for the electron-nuclear spin evolution,

$$\mathcal{H} = \gamma_S B S_z - \gamma_I B \sum_n I_{nz}$$

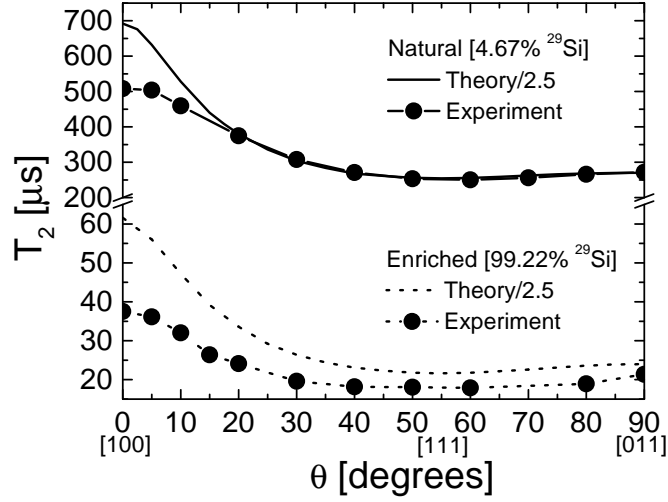


FIG. 1: Electron spin coherence time for a Si:P donor. θ denotes the angle between the external magnetic field and the [100] crystallographic direction. The agreement between theory and experiment is within a factor of 3 (experimental data from Ref. [27]).

$$\begin{aligned}
 & + \sum_n A_n I_{nz} S_z - 4 \sum_{n < m} b_{nm} I_{nz} I_{mz} \\
 & + \sum_{n < m} b_{nm} (I_{n+} I_{m-} + I_{n-} I_{m+}).
 \end{aligned} \tag{1}$$

Here S_z is the z-component of the electron spin operator, and γ_S is the electron gyromagnetic ratio. \mathbf{I}_n is the nuclear spin operator for a ^{29}Si isotope located at position \mathbf{R}_n , A_n is the hyperfine shift produced by this nucleus,

$$A_n = \gamma_S \gamma_I \hbar \frac{8\pi}{3} |\Psi(\mathbf{R}_n)|^2, \tag{2}$$

and b_{nm} is the dipolar coupling between two such nuclei,

$$b_{nm} = -\frac{1}{4} \gamma_I^2 \hbar \frac{1 - 3 \cos^2 \theta_{nm}}{R_{nm}^3}, \tag{3}$$

which has an important dependence with respect to the angle θ_{nm} between the magnetic field and the vector linking the two nuclei $\mathbf{R}_n - \mathbf{R}_m$. In Eq. (1) we neglect the off-diagonal hyperfine coupling ($S_+ I_{n-} + \text{h.c.}$), which can be shown to play no role at magnetic fields higher than the Overhauser field ($B > \sum_n A_n \sim 10 - 1000$ G in silicon [26]). The last term of Eq. (1) is responsible for flip-flop processes between two nuclear spins, which can be studied using an inverse temperature expansion. The rate for a flip-flop process is then given by [26]

$$\Gamma_{nm} = \frac{2\pi b_{nm}^2}{\sqrt{2\pi \kappa_{nm}^2}} \exp\left(-\frac{\Delta_{nm}^2}{2\kappa_{nm}^2}\right). \tag{4}$$

Here $\Delta_{nm} = |A_n - A_m|/2$ is the frequency shift felt by the electron when one flip-flop event takes place, while the linewidth for flip-flop is given by

$$\kappa_{nm}^2 = 4 \sum_{i \neq n, m} (b_{ni} - b_{mi})^2. \tag{5}$$

Nuclear spin flip-flop can only take place if the nuclear system can rearrange itself to compensate for the energy cost Δ_{nm} . Hence pairs of nuclei satisfying $\Delta_{nm} \gg \kappa_{nm}$ are inert. Since these are usually located close to the center of the donor (where A_n is larger), they form a frozen core which does not contribute appreciably to spectral diffusion.

An approximate theory for spectral diffusion decay can be obtained by assuming that the most important processes contributing to nuclear dipolar fluctuation are uncorrelated flip-flop transitions with Markovian dynamics. The

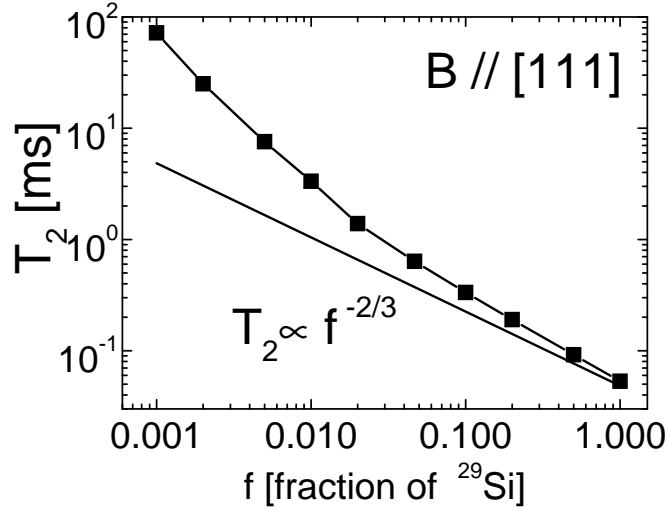


FIG. 2: Dependence of Si:P electron spin coherence time (as measured by Hahn echo decay) with the fraction of ^{29}Si nuclear spins. This figure reveals isotopic purification as an effective tool for material optimization of T_2 .

$\pi/2 - \tau - \pi - \tau - \text{echo}$ envelope arising due to the stochastic fluctuation of one pair of nuclei n, m is then determined to be [26]

$$v_{nm}(2\tau) = R_{nm}^{-2} e^{-2\tau\Gamma_{nm}} \left\{ \Gamma_{nm}^2 \cosh(2\tau R_{nm}) + \Gamma_{nm} R_{nm} \sinh(2\tau R_{nm}) - \Delta_{nm}^2 \right\}, \quad (6)$$

where $R_{nm}^2 = T_{nm}^{-2} - \Delta_{nm}^2$. We then consider the contribution of all nuclear spins through an averaged product

$$v(2\tau) = \prod_{n < m} [(1 - f^2) + f^2 v_{nm}(2\tau)], \quad (7)$$

where f is the fraction of ^{29}Si nuclear spins present in the lattice. Equation (7) allows realistic calculations of echo decay due to spectral diffusion without using any fitting parameters. All we need is an appropriate wave function for the electron (we use the Kohn-Luttinger state for a Si:P impurity) which in turn determines the hyperfine shifts Δ_{nm} and the corresponding fluctuation rates Γ_{nm} (other constants such as γ_S , γ_I are readily available from the NMR literature). For natural silicon, the calculated T_2 is 2.5 times larger than the measured value [21], a reasonable agreement in the spin relaxation literature [5]. In addition we were able to predict an important orientation dependence for T_2 (see Fig. 1). As the direction of the external magnetic field is changed with respect to the silicon diamond structure T_2 increases by as much as a factor of three. Recently, this prediction was verified experimentally for natural silicon [27, 28] and for a ^{29}Si enriched sample [27] (Fig. 1). The calculated dependence of T_2 on the fraction of ^{29}Si is shown in Fig. 2, establishing isotopic purification as an efficient way to achieve the longest possible electron spin coherence times for QC use. Recently A. M. Tyryshkin and collaborators [28] performed echo spectroscopy in a sample with less than 0.005% ^{29}Si isotopes. The residual $T_2 > 60$ ms was attributed to the lack of coherence in the applied ESR pulses, and not to the spectral diffusion process.

Isotopic purification can also be used in germanium, where the active nuclear spin is ^{73}Ge ($I = 9/2$, 7.73% natural abundance). On the other hand the important class of III-V semiconductors (GaAs, GaSb, InAs, InSb) has no known $I = 0$ nuclear isotopes. Because echo decay has never been measured for localized spins in these materials, the role of theory becomes extremely important. Recently we predicted $T_2 \sim 1 - 100 \mu\text{s}$ [25, 26] for localized electron spins in III-V semiconductor quantum dots, where the development of single spin detection techniques promises a bright future for coherent spin manipulations [29]. There are currently two proposals to reduce the effect of strong spectral diffusion associated with the absence of $I = 0$ isotopes in III-V materials. The first relies on substantial nuclear polarization [30] (very high nuclear polarization is required to suppress the flip-flop processes that lead to spectral diffusion [25]). The qualitative dependence of T_2 on nuclear polarization can be derived from the short τ limit of

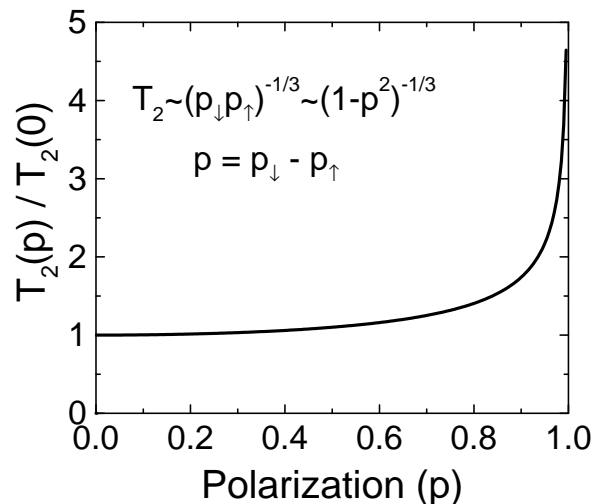


FIG. 3: Depicts the dependence of coherence time T_2 with the nuclear spin polarization p . Very high nuclear polarization ($p > 0.99$) is required to enhance T_2 , a condition which is very hard to achieve experimentally.

Eqs. (6) and (7). In this case we have [25]

$$\left(\frac{1}{T_2}\right)^3 \propto p_{\uparrow}p_{\downarrow} \propto (1-p^2), \quad (8)$$

where the nuclear spin polarization is given by $p = p_{\uparrow} - p_{\downarrow}$. This dependence implies T_2 is enhanced significantly only if p is very close to 1 (Fig. 3). For example, a nuclear polarization of $p = 99.5\%$ increases T_2 only by a factor of 5). The other approach to reduce spectral diffusion requires successive applications of π pulses (Carr-Purcell-Meiboom-Gill sequence) at a rate proportional to the square of the nuclear spin quantum number [31]. Both these proposals require considerable overhead, and make evident the advantages of silicon or germanium from the perspective of coherent spin manipulation.

We make two brief final comments before concluding our discussion of spin decoherence. The first comment is that we believe the spectral diffusion mechanism to be the ultimate decoherence mechanism for localized electron spins in semiconductor nanostructures since it cannot be eliminated in a given sample by reducing the sample temperature as the nuclear spin energy scale is extremely small (sub-millikelvins). Thus, understanding spectral diffusion effects in spin-based solid state QC architectures is one of the most important physics issues in the context of electron spin dynamics in quantum computers. From this narrow perspective, silicon QC has significant advantages over GaAs QC due to the unique role of isotopic purification in silicon. The second comment is that our statement about the spin coherence time in GaAs nanostructures (or more generally, in III-V materials) being ‘short’ ($T_2 \sim 1 - 100 \mu\text{s}$) should be understood in the proper context of a spectral diffusion comparison with the corresponding silicon coherence where $T_2 \sim 1 - 100 \text{ ms}$. In this context, recent claims in the literature of very long spin coherence times ($\sim 1\text{-}100 \text{ ns}$) in GaAs for conduction electrons are in fact extraordinarily short for the purpose of spin quantum computation.

III. DONOR ELECTRON EXCHANGE IN SILICON

An important issue in the study of donor-based Si QC architecture is coherent manipulations of spin states as required for the quantum gate operations. In particular, two-qubit operations, which are required for a universal QC, involve precise control over electron-electron exchange [7, 9, 11, 32] and electron-nucleus hyperfine interactions (for nuclear spin qubits). Such control can presumably be achieved by fabrication of donor arrays with accurate positioning and surface gates whose potential can be precisely controlled [33, 34, 35, 36]. However, electron exchange in bulk silicon has spatial oscillations [37, 38] on the atomic scale due to valley interference arising from the particular six-fold degeneracy of the bulk Si conduction band. These exchange oscillations place heavy burdens on device fabrication and coherent control [38], because of the very high accuracy and tolerance requirements for placing each donor inside the Si unit cell, and/or for controlling the external gate voltages.

The potentially severe consequences of the exchange-oscillation problem for exchange-based Si QC architecture motivated us and other researchers to perform theoretical studies going beyond some of the simplifying approximations

in the formalism adopted in Ref. 38, and incorporating perturbation effects due to applied strain[39] or gate fields [40]. These studies, all performed within the standard Heitler-London (HL) formalism [41], essentially reconfirm the originally reported difficulties regarding the sensitivity of the electron exchange coupling to precise atomic-level donor positioning, indicating that they may not be completely overcome by applying strain or electric fields. The sensitivity of the calculated exchange coupling to donor relative position originates from interference between the plane-wave parts of the six degenerate Bloch states associated with the Si conduction-band minima. More recently [42] we have assessed the robustness of the HL approximation for the two-electron donor-pair states by relaxing the phase pinning at donor sites, which could in principle eliminate the oscillatory exchange behavior. Within this more general theoretical scheme, the *floating-phase* HL approach, our main conclusion is that, for all practical purposes, the previously adopted HL wavefunctions are robust, and the oscillatory behavior obtained in Refs. 38, 39, 40 persists (quantitatively) in the more sophisticated theory of Ref. [42].

In what follows, we first review the main results leading to the exchange oscillation behavior qualitatively described above. We then consider two substitutional donors in bulk Si, and present a systematic statistical study of the correlation between the relative position distributions and the resulting exchange distributions. We also show that strain may partially alleviate the exchange oscillatory behavior, but it cannot entirely overcome it.

A. Donor Electron Exchange in Relaxed Bulk Silicon

We describe the single donor electron ground state using the effective mass theory. The bound donor electron Hamiltonian for an impurity at site \mathbf{R}_0 is written as

$$\mathcal{H}_0 = \mathcal{H}_{SV} + \mathcal{H}_{VO}. \quad (9)$$

The first term, \mathcal{H}_{SV} , is the single-valley Kohn-Luttinger Hamiltonian [43], which includes the single particle kinetic energy, the Si periodic potential, and the screened Coulomb perturbation potential produced by the impurity ion

$$V(\mathbf{r}) = -\frac{e^2}{\epsilon|\mathbf{r} - \mathbf{R}_0|}. \quad (10)$$

For shallow donors in Si, we use the static dielectric constant $\epsilon = 12.1$. The second term of Eq. (9), \mathcal{H}_{VO} , represents the inter-valley scattering effects due to the presence of the impurity.

The donor electron eigenfunctions are written in the basis of the six unperturbed Si band edge Bloch states $\phi_\mu = u_\mu(\mathbf{r})\mathbf{e}^{i\mathbf{k}_\mu \cdot \mathbf{r}}$ [recall that the conduction band of bulk Si has six degenerate minima ($\mu = 1, \dots, 6$), located along the Γ -X axes of the Brillouin zone at $|\mathbf{k}_\mu| \sim 0.85(2\pi/a)$ from the Γ point]:

$$\psi_{\mathbf{R}_0}(\mathbf{r}) = \frac{1}{\sqrt{6}} \sum_{\mu=1}^6 F_\mu(\mathbf{r} - \mathbf{R}_0) u_\mu(\mathbf{r}) e^{i\mathbf{k}_\mu \cdot (\mathbf{r} - \mathbf{R}_0)}. \quad (11)$$

The phases of the plane-wave part of all band edge Bloch states are naturally chosen to be pinned at \mathbf{R}_0 : In this way the charge density at the donor site [where the donor perturbation potential energy Eq. (10) is the smallest] is maximum, thus minimizing the energy for $\psi_{\mathbf{R}_0}(\mathbf{r})$.

In Eq. (11), $F_\mu(\mathbf{r} - \mathbf{R}_0)$ are envelope functions centered at \mathbf{R}_0 , for which we adopt the anisotropic Kohn-Luttinger form, e.g., for $\mu = z$, $F_z(\mathbf{r}) = \exp\{-(x^2 + y^2)/a^2 + z^2/b^2\}^{1/2}/\sqrt{\pi a^2 b}$. The effective Bohr radii a and b are variational parameters chosen to minimize $E_{SV} = \langle \psi_{\mathbf{R}_0} | \mathcal{H}_{SV} | \psi_{\mathbf{R}_0} \rangle$, leading to $a = 25 \text{ \AA}$, $b = 14 \text{ \AA}$ and $E_{SV} \sim -30 \text{ meV}$ when recently measured effective mass values are used in the minimization [38]. The periodic part of each Bloch function is pinned to the lattice, independent of the donor site.

The \mathcal{H}_{SV} ground state is six-fold degenerate due to the six-fold valley degeneracy of Si conduction band. This degeneracy is lifted by the valley-orbit interactions [44], which are included here in \mathcal{H}_{VO} , leading to the nondegenerate (A_1 -symmetry) ground state in (11).

The HL approximation is a reliable scheme for the well-separated donor pair problem (interdonor distance much larger than the donor Bohr radii) [41]. Within HL, the lowest energy singlet and triplet wavefunctions for two electrons bound to a donor pair at sites \mathbf{R}_A and \mathbf{R}_B , are written as properly symmetrized combinations of $\psi_{\mathbf{R}_A}$ and $\psi_{\mathbf{R}_B}$ [as defined in Eq.(11)]

$$\Psi_t^s(\mathbf{r}_1, \mathbf{r}_2) = \frac{1}{\sqrt{2(1 \pm S^2)}} [\psi_{\mathbf{R}_A}(\mathbf{r}_1)\psi_{\mathbf{R}_B}(\mathbf{r}_2) \pm \psi_{\mathbf{R}_B}(\mathbf{r}_1)\psi_{\mathbf{R}_A}(\mathbf{r}_2)], \quad (12)$$

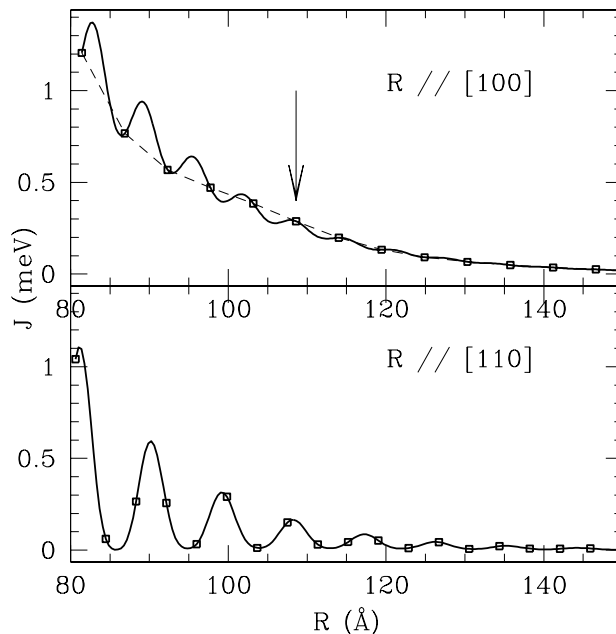


FIG. 4: Exchange coupling between two phosphorus donors in Si along the indicated directions in the diamond structure. Values appropriate for impurities at substitutional sites are given by the squares. The dashed line in the $R \parallel [100]$ frame is a guide to the eye, indicating that the oscillatory behavior may be ignored for donors positioned exactly along this axis.

where S is the overlap integral and the upper (lower) sign corresponds to the singlet (triplet) state. The energy expectation values for these states, $E_t^s = \langle \Psi_t^s | \mathcal{H} | \Psi_t^s \rangle$, give the exchange splitting through their difference, $J = E_t - E_s$. We have previously derived the expression for the donor electron exchange splitting [39, 42], which we reproduce here:

$$J(\mathbf{R}) = \frac{1}{36} \sum_{\mu, \nu} \mathcal{J}_{\mu\nu}(\mathbf{R}) \cos(\mathbf{k}_\mu - \mathbf{k}_\nu) \cdot \mathbf{R}, \quad (13)$$

where $\mathbf{R} = \mathbf{R}_A - \mathbf{R}_B$ is the interdonor position vector and $\mathcal{J}_{\mu\nu}(\mathbf{R})$ are kernels determined by the envelopes and are slowly varying [38, 39]. Note that Eq. (13) does not involve any oscillatory contribution from $u_\mu(\mathbf{r})$, the periodic part of the Bloch functions [40, 42]. The physical reason for that is clear from (11): While the plane-wave phases of the Bloch functions are pinned to the donor sites, leading to the cosine factors in (13), the periodic functions u_μ are pinned to the lattice, regardless of the donor location.

The exchange energy calculated from Eq. (13) for a pair of donors as a function of their relative position along the [100] and [110] crystal axis is given in Fig. 4. This figure vividly illustrates both the anisotropic and the oscillatory behavior of $J(\mathbf{R})$, which is well established from previous studies [37, 38, 39, 40]. It is interesting to note that for substitutional donors with interdonor position vectors exactly aligned with the [100] crystal axis, the oscillatory behavior may be ignored in practice, as indicated by the dashed line in the figure. This behavior is qualitatively similar to the exchange versus donor separation dependence assumed in Kane's proposal [9], where the Herring and Flicker expression [45], originally derived for H atoms, was adapted for donors in Si. Therefore one might expect that reliable exchange gate operations would be possible if all donor pairs are exactly aligned along the [100] crystal axis.

B. Nanofabrication aspects

Aiming at the fabrication of a P donor array accurately positioned along the [100] axis, and taking into account the current state of the arts degree of control in substitutional P positioning in Si of a few nm [33, 34, 35, 36], we investigate the consequences of such interdonor positioning uncertainties (\sim a few nm) in the values of the corresponding pairwise

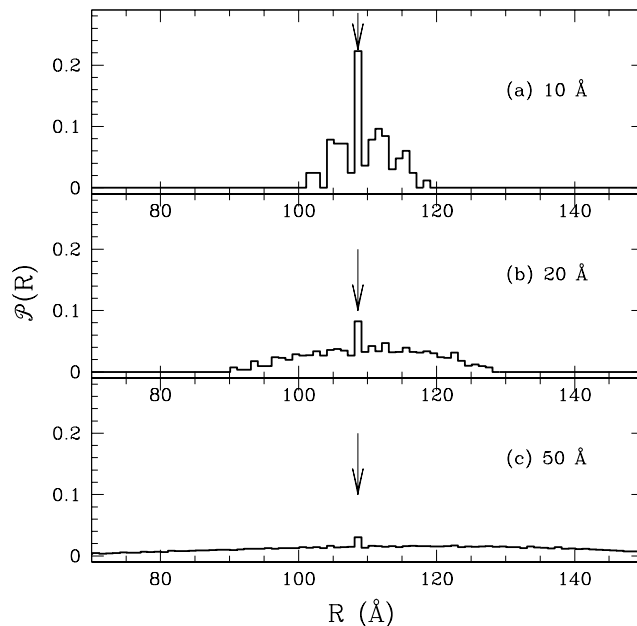


FIG. 5: Interdonor distance distributions for a *target* relative position of 20 lattice parameters along [100] (see arrows). The first donor is fixed and the second one “visits” all of the Si substitutional lattice sites within a sphere centered at the *target* position, with uncertainty radii (a) 10 Å, (b) 20 Å and (c) 50 Å.

exchange coupling. We define the *target* interdonor position \mathbf{R}_t along [100], with an arbitrarily chosen length of 20 lattice constants (~ 108.6 Å) indicated by the arrow in Fig. 4. The distributions for the interdonor distances $R = |\mathbf{R}_A - \mathbf{R}_B|$ when \mathbf{R}_A is fixed and \mathbf{R}_B “visits” all of the diamond lattice sites within a sphere centered at the *target* position are given in Fig. 5. Different frames give results for different uncertainty radii, and, as expected, increasing the uncertainty radius results in a broader distribution around the *target* distance. Note that the geometry of the lattice implies that the distribution is always centered and peaked around R_t , as indicated by the arrows. The additional peaks in the distribution reveal the discrete nature of the Si lattice.

The respective distributions of exchange coupling between the same donor pairs in each *ensemble* is presented in Fig. 6, where the arrows give the exchange value at the *target* relative position: $J(\mathbf{R}_t) \sim 0.29$ meV. The results here are qualitatively different from the distance distributions in Fig. 5, since they are neither centered nor peaked at the *target* exchange value. Even for the smallest uncertainty radius of 1 nm in (a), the exchange distribution is peaked around $J \sim 0$, bearing no semblance to the inter-donor distance distributions. Increasing the uncertainty radius leads to a wider range of exchange values, with a more pronounced peak around the lowest J values.

From the perspective of current QC fabrication efforts, ~ 1 nm accuracy in single P atom positioning has been recently demonstrated [34], representing a major step towards the goal of obtaining a regular donor array embedded in single crystal Si. Distances and exchange coupling distributions consistent with such accuracy are presented in Figs. 5(a) and 6(a) respectively. The present calculations indicate that even such small deviations (~ 1 nm) in the relative position of donor pairs with respect to perfectly aligned substitutional sites along [100] lead to order-of-magnitude changes in the exchange coupling, favoring $J \sim 0$ values. Severe limitations in controlling J would come from “hops” into different substitutional lattice sites. Therefore, precisely controlling of exchange gates in Si remains an open (and severe) challenge.

C. Strained Si

Uniaxial strain can be used to break the Si lattice symmetry and partially lift the degeneracy between the valleys, so that as few as two valleys make up the bottom of the conduction band. Then the sum over μ and ν in Eq. (13)

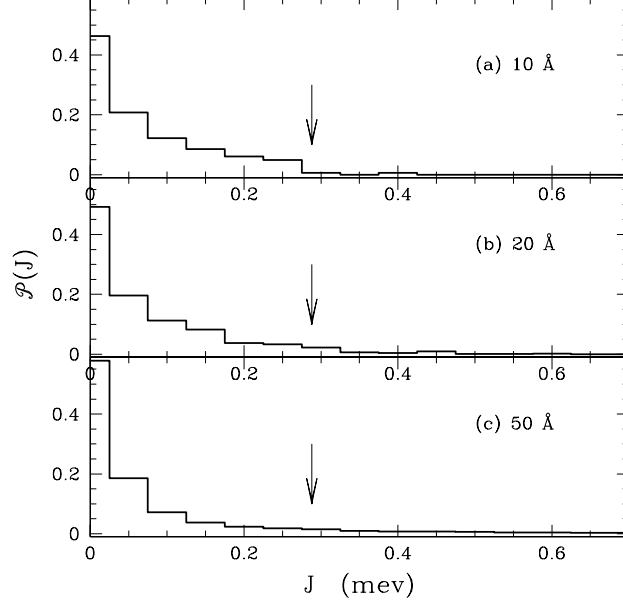


FIG. 6: Exchange distributions for the same relative position *ensembles* in Fig. 5. The arrow indicates the *target* situation. Contrary to the distance distributions, the exchange distributions are not centered or peaked around the target value.

is much simplified, but the sinusoidal factor will still remain, so that care still has to be taken in controlling the donor exchange [39]. For example, if a uniaxial strain is applied along z direction, variation of relative donor position in the x - y plane does not lead to oscillation in the inter-donor exchange, as shown in Fig. 7. Strain is quantified here by a dimensionless parameter, χ , defined in Ref. [39]. On the other hand, atomic scale donor movement in a direction parallel to the strain direction z can still cause order-of-magnitude change in the donor exchange coupling, as is illustrated in Fig. 8. Therefore the exchange oscillation problem (leading to essentially random variations in the exchange coupling arising from dopant positioning within the Si unit cell) remains even in uniaxially strained Si since the system still has a two-valley degeneracy. These theoretical considerations [39] have recently been verified in a more sophisticated approximation which took into account higher-order Coulomb interaction corrections [40].

Given the random variations in the exchange energy as a function of unintentional (and unavoidable at present) small (~ 1 nm) variations in the positioning of P dopants in Si unit cell, as shown in Figs. 4-8, a careful rethinking of the exchange gate fabrication and control for Si QC architecture may be required. This is particularly true in view of the fundamental origin of the exchange oscillations, which arises from the quantum interference between the degenerate valleys in the silicon conduction band and therefore cannot be eliminated by simple fabrication tools (unless, of course, dopant positioning with sub-nanometer precision on the Si lattice somehow becomes available). One possibility is to eliminate the use of exchange gates and instead rely completely on hyperfine coupling and electron shuttling [46]. Another possibility could be to go away completely from shallow donor bound states in Si and instead use SiGe quantum dot structures to confine single electrons, making the Si QC essentially identical to the proposed GaAs quantum dot QC [47]. Even in this case, however, the valley degeneracy problem may remain unless the quantum dot confinement potential is extremely weak (which would cause other problems such as the low lying orbital excited states potentially jeopardizing the two-level dynamics of the spin qubit). In any case, our results of the strong (essentially random) qubit-to-qubit variations in the exchange energy in the P-doped shallow-donor-based Si QC architecture compromises one of the main perceived advantages of Si QC (over, for example, the GaAs quantum dot QC), namely, the identical nature of each spin qubit (arising from all P shallow donor states in Si being identical by definition) does not seem to translate to similar exchange gate characteristics—in fact, the exchange gate turns out to be essentially random in nature (with wide variations in its strength peaking at zero).

Comparing with Si, a question naturally arises about the GaAs quantum dot QC where the exchange would also exhibit random qubit-to-qubit variations arising from the (essentially trivial) random variations ($\pm 10\%$ - 20%) in

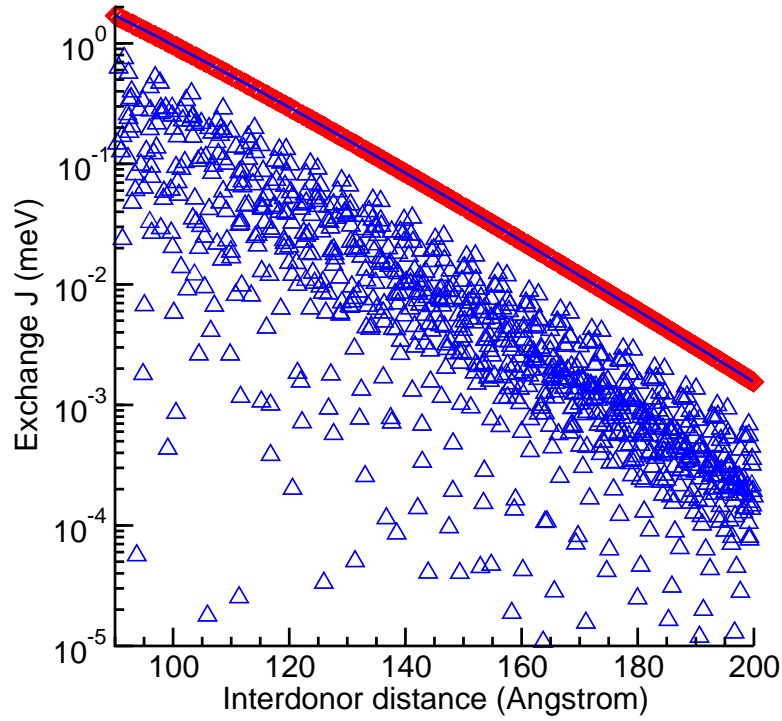


FIG. 7: Calculated exchange coupling for in-plane displacements of the donors in the x - y plane for relaxed Si ($\chi = 0$, with diamond symbols) and strained Si (uniaxial strain along the z direction with $\chi = -20$, with square symbols forming a straight line). The relative positions considered for the donor pairs consist of one donor at all possible lattice sites between two concentric circles of radii 90 Å and 180 Å with the other donor positioned at the center of the circles. The data points correspond to the exchange calculated at all relative positions considered. The solid line is $J(\mathbf{R})$ for \mathbf{R} along the $[100]$ direction for $\chi = -20$.

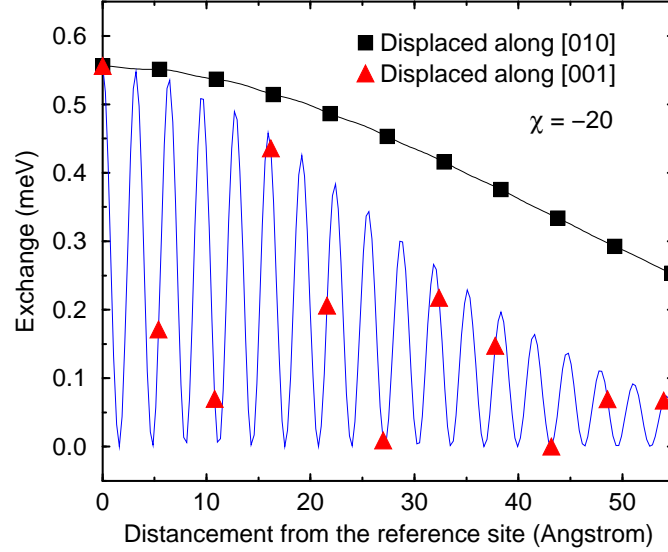


FIG. 8: Donor electron exchange splitting in Si uniaxially strained along $[001]$ direction ($\chi = -20$, corresponding to the strain in a Si quantum well grown in between relaxed $\text{Si}_{0.8}\text{Ge}_{0.2}$ barriers). The two donors are approximately aligned along the $[100]$ direction, with one of them displaced along the $[010]$ direction (original figure appeared in Ref. 39).

quantum dot confinement sizes and inter-dot separations since it is impossible to fabricate identical quantum dots and/or to place them perfectly in an architecture. The quantum dot exchange variation problem (arising in the leading order from the $e^{-R/a}$ sensitivity of the exchange energy of the inter-dot separation R) is, however, less severe because the “random” exchange in this case will be peaked around a finite value in contrast to Si QC, where the most probable value of the inter-qubit exchange coupling is zero. We note, however, that in both cases one may have to carry out extensive characterization of the individual qubit-to-qubit coupling strength in order to operate the exchange gate, and such qubit characterization itself may turn out to be a hard control problem. We have recently proposed an experimental technique of spatially resolved micro-Raman spectroscopy as possible diagnostic tool to characterize local values of exchange coupling between individual spin qubits (i.e. the singlet-triplet energy splitting for individual pairs of induced shallow electron donor states) [48].

IV. SUMMARY

In summary, we have briefly reviewed two important issues related to donor-spin based quantum computing in silicon: quantum coherence of electron spins and exchange interaction among donor electrons. Our results show that the spin qubits based on donors in silicon have remarkable potential for very long quantum coherence times through isotopic purification. On the other hand, they also pose immense challenges in terms of precise nanostructure fabrications because of the degenerate nature of the silicon conduction band, which leads to essentially a random exchange gate coupling. Further studies of fabrication and innovative alternative approaches are imperative in order to fully realize the potential of this donor-based QC architecture. We have discussed an interesting dichotomy between donor-based Si and quantum dot-based GaAs QC architectures. In particular, isotopic purification, which can eliminate essentially all free nuclear spins (by eliminating ^{29}Si nuclei) in silicon (but not in GaAs), gives Si an enormous advantage of very long ($T_2 \gtrsim 10 - 100$ ms) electron spin decoherence time compared with the corresponding GaAs quantum dot situation ($T_2 \sim 10 - 100$ μs , three orders of magnitude shorter than in Si), making Si an ideal QC candidate material. However, the valley degeneracy of Si conduction band leads to demands for extremely precise dopant positioning (so that the inter-qubit exchange coupling is finite for most qubits) which will be difficult to achieve. It may be worthwhile in this context to consider alternative two-qubit gates, such as the dipolar gate [16] or electron shuttling [46], for silicon quantum computation.

Acknowledgments

This work was supported by ARDA and LPS-NSA, as well as by CNPq, Instituto do Milênio de Nanociências and FAPERJ in Brazil, by ARO-ARDA at the University at Buffalo and the University of Maryland, and by DARPA SpinS program at the University of California at Berkeley.

-
- [1] M.A. Nielsen and I.L. Chuang, “Quantum computation and quantum information” (Cambridge Univ. Press, Cambridge, U.K., 2000).
 - [2] D.P. DiVincenzo, “Quantum Computation,” *Science* **270** (1995) 255; A. Ekert and R. Jozsa, “Quantum computation and Shor’s factoring algorithm,” *Rev. Mod. Phys.* **68** (1996) 733; A. Steane, “Quantum computing,” *Rep. Prog. Phys.* **61** (1998) 117; C.H. Bennett and D.P. DiVincenzo, “Quantum information and computation,” *Nature* **404** (2000) 247.
 - [3] P.W. Shor, “Polynomial-time algorithms for prime factorization and discrete logarithms on a quantum computer,” in: S. Goldwasser ed., *Proceedings of the 35th Annual Symposium on the Foundations of Computer Science* (IEEE Computer Society, Los Alamitos, 1994), 124-134.
 - [4] P.W. Shor, “Scheme for reducing decoherence in quantum computer memory,” *Phys. Rev A* **52** (1995), R2493-R2496; A.M. Steane, Error correcting codes in quantum theory, *Phys. Rev. Lett.* **77** (1996) 793-797.
 - [5] I. Žutić, J. Fabian, and S. Das Sarma, “Spintronics: Fundamentals and applications,” *Rev. Mod. Phys.* **76** (2004) 323.
 - [6] S. Das Sarma, J. Fabian, I. Žutić, “Spin electronics and spin computation,” *Solid State Commun.* **119** (2001) 207; X. Hu and S. Das Sarma, “Overview of spin-based quantum dot quantum computation,” *Phys. Stat. Sol. (b)* **238** (2003) 260; X. Hu, “Quantum Dot Quantum Computing,” *cond-mat/0411012*.
 - [7] D. Loss and D. P. DiVincenzo, “Quantum computation with quantum dots,” *Phys. Rev. A* **57** (1998) 120.
 - [8] A. Imamoglu, D.D. Awschalom, G. Burkard, D.P. DiVincenzo, D. Loss, M. Sherwin, and A. Small, “Quantum information processing using quantum dot spins and cavity QED,” *Phys. Rev. Lett.* **83** (1999) 4204-4207.
 - [9] B.E. Kane, “A silicon-based nuclear spin quantum computer,” *Nature* **393** (1998) 133.
 - [10] V. Privman, I.D. Vagner, and G. Kventsel, “Quantum computation in quantum-Hall systems,” *Phys. Lett. A* **239** (1998) 141-146.

- [11] R. Vrijen, E. Yablonovitch, K. Wang, H.W. Jiang, A. Balandin, V. Roychowdhury, Tal Mor, and D.P. DiVincenzo, "Electron-spin-resonance transistors for quantum computing in silicon-germanium heterostructures," *Phys. Rev. A* **62** (2000) 012306.
- [12] P.M. Voyles, D.A. Muller, J.L. Grazui, P.H. Citrin, and H.-J.L. Grossmann, "Atomic-scale imaging of individual dopant atoms and clusters in highly n-type bulk Si," *Nature* **416** (2002) 826.
- [13] T. Tanamoto, "One- and two-dimensional N-qubit systems in capacitively coupled quantum dots", *Phys. Rev. A* **64** (2001) 062306; "Quantum gates by coupled asymmetric quantum dots and controlled-NOT-gate operation", *ibid.* **61** (2000) 022305.
- [14] *Single Charge Tunneling*, ed. by H. Grabert and M.H. Devoret (Plenum, New York, 1992).
- [15] M.I. Dykman, F.M. Izrailev, L.F. Santos, and M. Shapiro, "Many-particle localization by constructed disorder: enabling quantum computing with perpetually coupled qubits", *cond-mat/0401201*.
- [16] R. de Sousa, J.D. Delgado, and S. Das Sarma, "Silicon quantum computation based on magnetic dipolar coupling", *Phys. Rev. A* **70** (2004) 052304.
- [17] X. Hu and S. Das Sarma, "Gate errors in solid state quantum computation," *Phys. Rev. A* **66** (2002) 012312.
- [18] A. Abragam, "The Principles of Nuclear Magnetism" (Oxford University Press, London, 1961); C.P. Slichter, "Principles of Magnetic Resonance" (Springer-Verlag, Berlin, 1996); X. Hu, R. de Sousa, and S. Das Sarma, "Decoherence and dephasing in spin-based solid state quantum computers", in the Proceedings for the 7th International Symposium on Foundations of Quantum Mechanics in the Light of New Technology, Saitama, Japan (August, 2001), ed. by Y.A. Ono and J. Fujikawa (World Scientific, River Edge, 2002). An extended version available at *cond-mat/0108339*.
- [19] Y. Yafet, "g-factors and spin-lattice relaxation of conduction electrons", in *Solid State Physics*, Vol. **14**, Ed. by F. Seitz and D. Turnbull (Academic, New York), p. 2 (1963).
- [20] G. Feher and E.A. Gere, "Electron spin resonance experiments on donors in silicon. II. Electron spin relaxation effects", *Phys. Rev.* **114** (1959) 1245.
- [21] M. Chiba and A. Hirai, "Electron spin echo decay behaviors of phosphorus doped silicon", *J. Phys. Soc. Japan* **33** (1972) 730.
- [22] D. Pines, J. Bardeen, and C.P. Slichter, "Nuclear polarization and impurity-state relaxation processes in silicon", *Phys. Rev.* **106** (1957) 489.
- [23] C. Tahan, M. Friesen, and R. Joynt, "Decoherence of electron spin qubits in Si-based quantum computers", *Phys. Rev. B* **66** (2002) 035314.
- [24] B. Herzog and E.L. Hahn, "Transient nuclear induction and double nuclear resonance in solids", *Phys. Rev.* **103** (1956) 148; J.P. Gordon and K.D. Bowers, "Microwave Spin Echoes from Donor Electrons in Silicon", *Phys. Rev. Lett.* **1** (1958) 368; W.B. Mims, K. Nassau, and J.D. McGee, "Spectral diffusion in spin resonance lines", *Phys. Rev.* **123** (1961) 2059; J.R. Klauder and P.W. Anderson, "Spectral diffusion decay in spin resonance experiments", *ibid.* **125** (1962) 912.
- [25] R. de Sousa and S. Das Sarma, "Electron spin coherence in semiconductors: Considerations for a spin-based solid-state quantum computer architecture", *Phys. Rev. B* **67** (2003) 033301.
- [26] R. de Sousa and S. Das Sarma, "Theory of nuclear-induced spectral diffusion: Spin decoherence of phosphorus donors in Si and GaAs quantum dots", *Phys. Rev. B* **68** (2003) 115322.
- [27] E. Abe, K.M. Itoh, J. Isoya, and S. Yamasaki, "Electron-spin phase relaxation of phosphorus donors in nuclear-spin-enriched silicon", *Phys. Rev. B* **70** (2004) 033204.
- [28] A.M. Tyryshkin, S.A. Lyon, A.V. Astashkin and A.M. Raitsimring, "Electron spin relaxation times of phosphorus donors in silicon", *Phys. Rev. B* **68** (2003) 193207.
- [29] J.M. Elzerman, R. Hanson, L.H.W. van Beveren, B. Witkamp, L.M.K. Vandersypen, and L.P. Kouwenhoven, "Single-shot read-out of an individual electron spin in a quantum dot", *Nature* **430** (2004) 431.
- [30] G. Burkard, D. Loss, and D.P. DiVincenzo, "Coupled quantum dots as quantum gates", *Phys. Rev. B* **59** (1999) 2070; A.V. Khaetskii, D. Loss, and L. Glazman, "Electron Spin Decoherence in Quantum Dots due to Interaction with Nuclei", *Phys. Rev. Lett.* **88** (2002) 186802; D. Gammon, A.L. Efros, T.A. Kennedy, M. Rosen, D.S. Katzer, D. Park, S. W. Brown, V. L. Korenev, and I. A. Merkulov, "Electron and Nuclear Spin Interactions in the Optical Spectra of Single GaAs Quantum Dots", *ibid.* **86** (2001) 5176; A. Imamoglu, E. Knill, L. Tian, and P. Zoller, "Optical Pumping of Quantum-Dot Nuclear Spins", *ibid.* **91** (2003) 017402; K. Ono and S. Tarucha, "Nuclear-Spin-Induced Oscillatory Current in Spin-Blockaded Quantum Dots", *ibid.* **92** (2004) 256803.
- [31] R. de Sousa, N. Shenvi, and K. B. Whaley, "Qubit coherence control in a nuclear spin bath", *cond-mat/0406090*.
- [32] X. Hu and S. Das Sarma, "Hilbert-space structure of a solid-state quantum computer: Two-electron states of a double-quantum-dot artificial molecule," *Phys. Rev. A* **61** (2000) 062301.
- [33] J.L. O'Brien, S.R. Schofield, M.Y. Simmons, R.G. Clark, A.S. Dzurak, N.J. Curson, B.E. Kane, N.S. McAlpine, M.E. Hawley, and G.W. Brown, "Towards the fabrication of phosphorus qubits for a silicon quantum computer," *Phys. Rev. B* **64** (2001) 161401.
- [34] S.R. Schofield, N.J. Curson, M.Y. Simmons, F.J. Rueß, T. Hallam, L. Oberbeck, and R.G. Clark, "Atomically precise placement of single dopants in Si," *Phys. Rev. Lett.* **91** (2003) 136104.
- [35] T.M. Buehler, R.P. McKinnon, N.E. Lumpkin, R. Brenner, D.J. Reilly, L.D. Macks, A.R. Hamilton, A.S. Dzurak, and R.G. Clark, "A self-aligned fabrication process for silicon quantum computer devices," *Nanotechnology* **13** (2002) 686.
- [36] T. Schenkel, A. Persaud, S.J. Park, J. Nilsson, J. Bokor, J.A. Liddle, R. Keller, D.H. Schneider, D.W. Cheng, and D.E. Humphries, "Solid state quantum computer development in silicon with single ion implantation," *Journal of Applied Physics* **94** (2003) 7017.
- [37] K. Andres, R.N. Bhatt, P. Goalwin, T.M. Rice, and R.E. Walstedt, "Low-temperature magnetic-susceptibility of Si-P in

- the non-metallic region,” Phys. Rev. B **24** (1981) 244.
- [38] B. Koiller, X. Hu and S. Das Sarma, “Exchange in silicon-based quantum computer architecture,” Phys. Rev. Lett. **88** (2002) 027903.
 - [39] B. Koiller, X. Hu and S. Das Sarma, “Strain effects on silicon donor exchange: Quantum computer architecture considerations,” Phys. Rev. B **66** (2002) 115201.
 - [40] C.J. Wellard, L.C.L. Hollenberg, F. Parisoli, L. Kettle, H.-S. Goan, J.A.L. McIntosh, and D.N. Jamieson, “Electron exchange coupling for single-donor solid-state spin qubits,” Phys. Rev. B **68** (2003) 195209.
 - [41] J. C. Slater, *Quantum Theory of Molecules and Solids*, vol. 1, McGraw-Hill, New York, 1963.
 - [42] B. Koiller, R.B. Capaz, X. Hu and S. Das Sarma, “Shallow donor wavefunctions and donor-pair exchange in silicon: Ab initio theory and floating-phase Heitler-London approach,” arXiv:cond-mat/0402266, Phys. Rev. B **70** (2004) 115207.
 - [43] W. Kohn, “Shallow impurity states in silicon and germanium,” in *Solid State Physics*, vol. 5, F. Seitz and D. Turnbull Ed. New York: Academic Press, 1957, pp. 257-320.
 - [44] S.T. Pantelides, “The electronic structure of impurities and other point defects in semiconductors,” Rev. Mod. Phys. **50** (1978) 797.
 - [45] C. Herring and M. Flicker, “Asymptotic Exchange Coupling of Two Hydrogen Atoms,” Phys. Rev. **134** (1964) A362.
 - [46] A.J. Skinner, M.E. Davenport, and B.E. Kane, “Hydrogenic spin quantum computing in silicon: A digital approach”, Phys. Rev. Lett. **90** (2003) 087901.
 - [47] M. Friesen, P. Rugheimer, D.E. Savage, M.G. Lagally, D.W. van der Weide, R. Joynt, and M.A. Eriksson, “Practical design and simulation of silicon-based quantum-dot qubits”, Phys. Rev. B **67** (2003) 121301.
 - [48] B. Koiller, X. Hu, H.D. Drew, and S. Das Sarma, “Disentangling the Exchange Coupling of Entangled Donors in the Silicon Quantum Computer Architecture”, Phys. Rev. Lett. **90** (2003) 067401.